Supporting Information

Enhanced stretchability of metal/interlayer/metal hybrid electrode

Seungseok Han,[‡a] Ki-Won Seo,[‡a] Wansun Kim,[b] Taek-Soo Kim,[b] and Jung-Yong Lee*,[a]

[a]School of Electrical Engineering (EE), Korea Advanced Institute of Science and Technology (KAIST), Daejeon 34141, Republic of Korea

[b]Department of Mechanical Engineering, Korea Advanced Institute of Science and Technology (KAIST), Daejeon 34141, Republic of Korea

Optimal interlayer thickness of PEDOT:PSS or CNT in the SHEs

Fig. S1 shows the optimal interlayer thickness of PEDOT:PSS or CNT in the SHEs. When using the same silver (Ag) thin film thickness (20 nm), the resistance change decreased as the interlayer thickness increased. The optimal thickness of both the PEDOT:PSS and CNT interlayers was 120 nm.

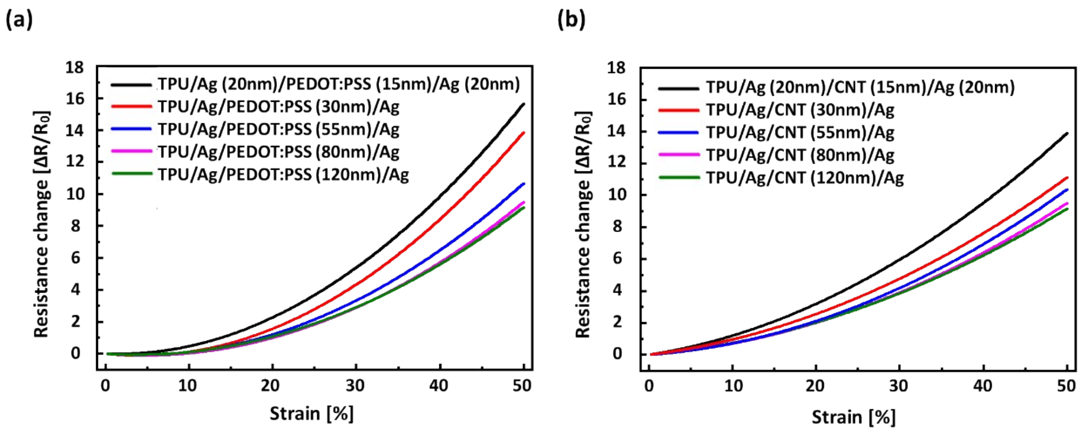

Fig. S1. Resistance changes in stretchable hybrid electrode (SHE) with (a) poly(3,4-ethylenedioxythiophene):poly(styrenesulfonate) (PEDOT:PSS) and (b) carbon nanotube (CNT) interlayers with increasing interlayer thickness during a tensile test.

Tensile test images by in-situ SEM of SHE-P and SHE-C

Fig. S2 shows tensile test images by in-situ SEM of SHE-P and SHE-C from 0% strain to 50% strain. These SEM images show that the crack develops gradually by the strain increases.

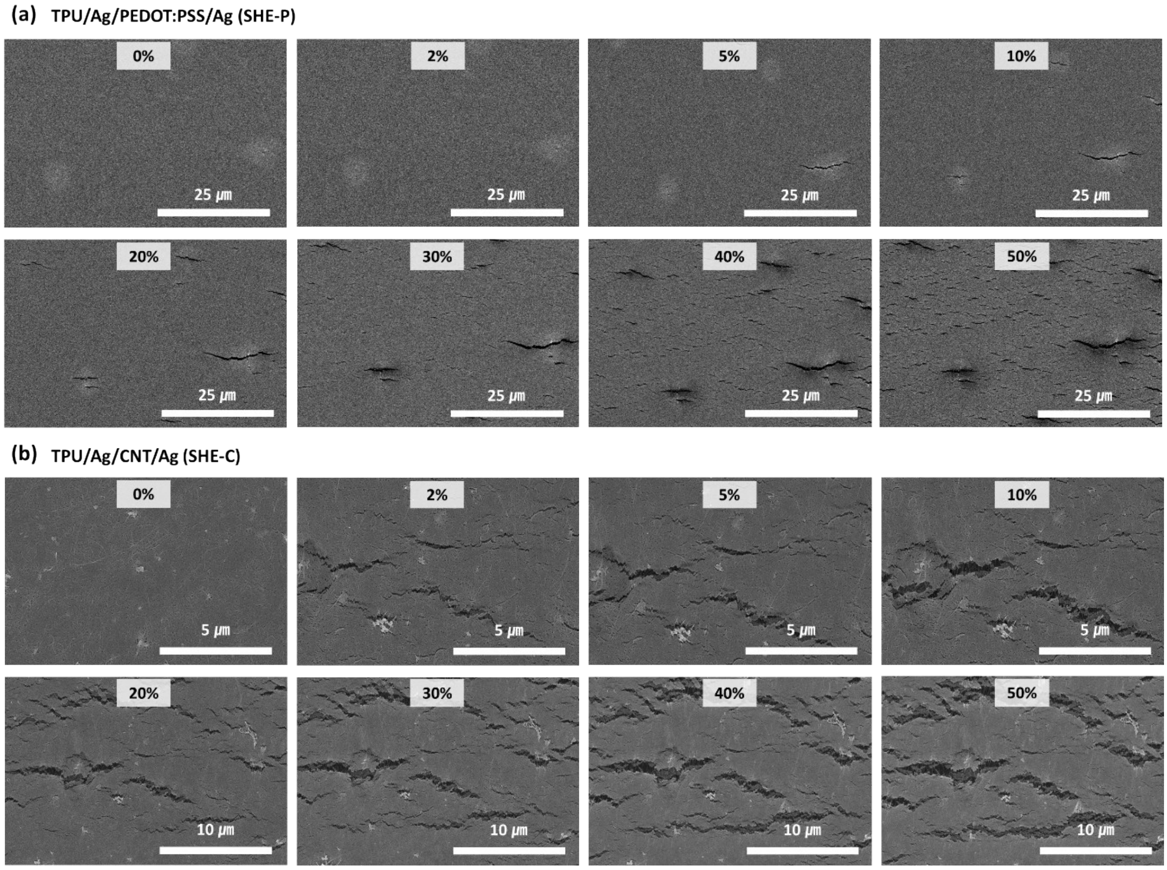

Fig. S2. Tensile test images by in-situ SEM of (a) SHE-P and (b) SHE-C from 0% to 50% strain.

Resistance and crack areal density of SHE-P and SHE-C

Fig. S3(a) shows the resistance change of SHE-P and SHE-C as a function of the crack areal density. Figure S3 (b) and (c) show the rates of resistance and crack areal density under an applied strain, respectively.

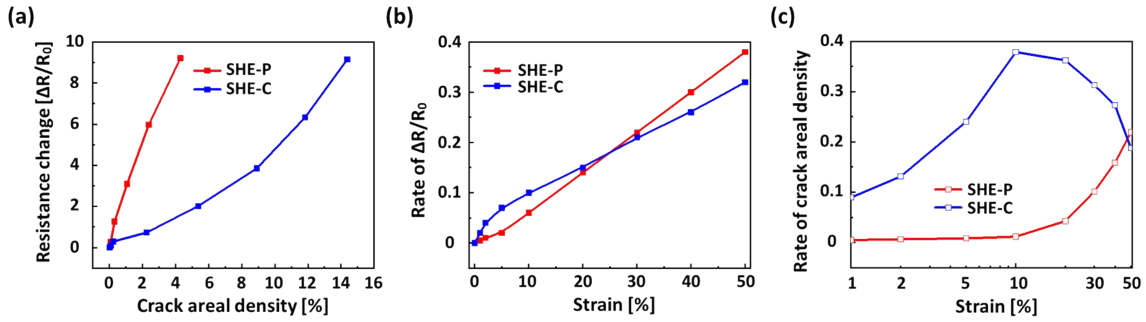

Fig. S3. (a) The resistance change of SHEs as a function of the crack areal density. The rates of the resistance change (b) and the crack areal density (c) of SHEs under strain.

Stress-strain curve of 20 nm-thick Ag thin film and atomic force microscope image for mechanical simulations

Fig. S24(a) shows stress–strain curve of a 20 nm Ag thin film for finite element mechanical simulation analysis. The free-standing sample on water method was utilized to measure the mechanical properties of the metal thin film.[1] We obtained the mechanical properties (i.e., Young's modulus and maximum tensile stress) of the 20 nm-thick Ag thin film from the free-standing sample, as illustrated in Fig. S24(a). Fig. S24(b) and S24(c) illustrate the surface morphologies (i.e., step height image and section profile) of PEDOT:PSS and CNT inserted SHEs, respectively.

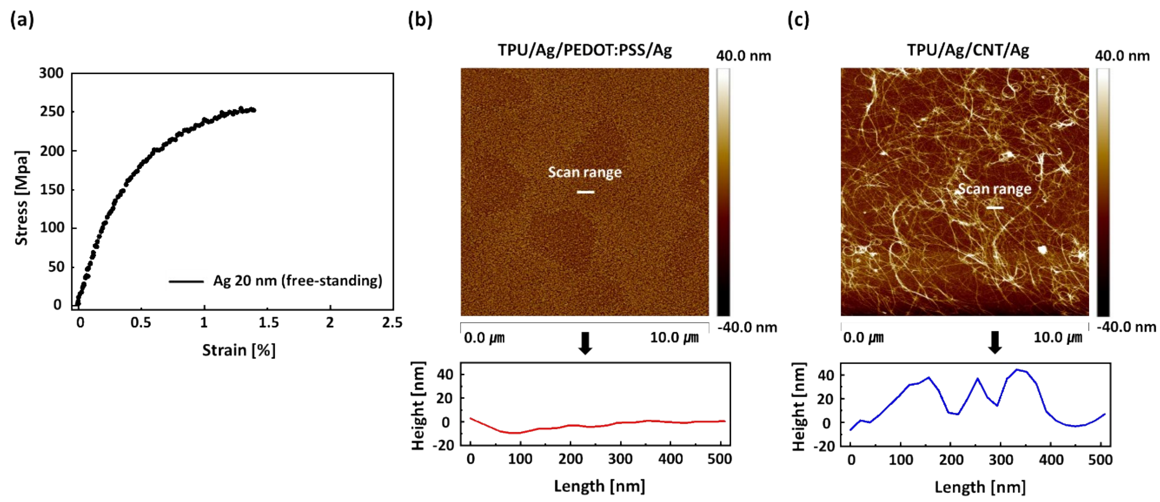

Fig. S24. (a) Stress–strain curve of 20 nm-thick Ag thin film obtained from a free-standing sample on water. (b) Surface profile and cross-section height profile of thermoplastic polyurethane (TPU)/Ag/PEDOT:PSS/Ag and TPU/Ag/CNT/Ag by atomic force microscope (AFM).

Bi-axial crack pattern of TPU/Ag/air/Ag film

Fig. S5 shows SEM images of the bi-axial crack pattern of a TPU/Ag/air/Ag film. This is because when the thin film is stretched, compression occurs in the perpendicular direction to the stretch owing to positive Poisson effect. This compression forms a buckling in the thin film, and as a result, cracks.[2-4] Indeed, in our TPU/Ag/air/Ag, crack-widening occurred along the stretching direction, but wrinkles were observed along the perpendicular direction of stretching.

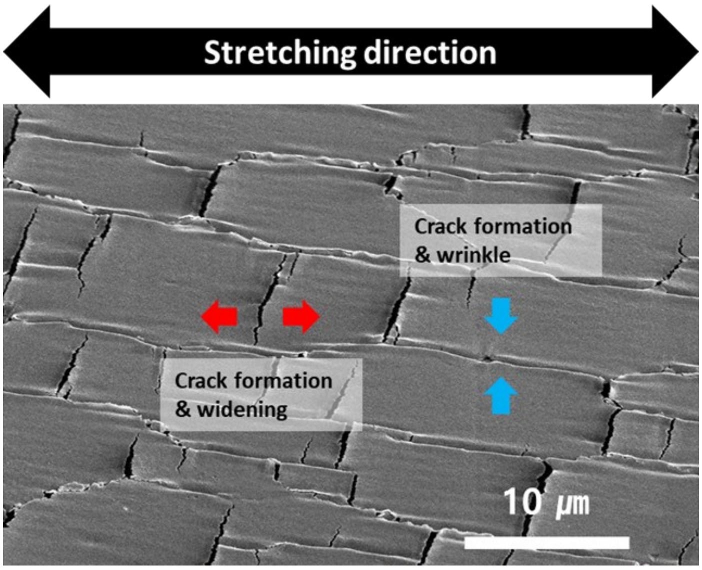

Fig. S5. Bi-axial crack formation in a TPU/Ag/air/Ag film. Cracks are widened along the stretching direction, and wrinkles are formed along the perpendicular direction of stretching.

Reference

1. J. H. Kim, A. Nizami, Y. Hwangbo, B. Jang, H. J. Lee, C. S. Woo, S. Hyun and T. S. Kim, *Nature Communications*, 2013, **4**, 2520.
2. C. Zhang, F. L. Chen, M. H. Gray, R. Tirawat and R. E. Larsen, *International Journal of Solids and Structures*, 2017, **120**, 125-136.
3. V. M. Marx, C. Kirchlechner, I. Zizak, M. J. Cordill and G. Dehm, *Philosophical Magazine*, 2015, **95**, 1982-1991.
4. V. M. Marx, F. Toth, A. Wiesinger, J. Berger, C. Kirchlechner, M. J. Cordill, F. D. Fischer, F. G. Rammerstorfer and G. Dehm, *Acta Materialia*, 2015, **89**, 278-289.